euspen's 24th International Conference & Exhibition, Dublin, IE, June 2024
www.euspen.eu

High-precision flexure-based XY-stage with high stiffness and load capacity

Patrick Flückiger[1], Hubert Schneegans[1], Simón Prêcheur Llarena[1], Charles Baur[1], Simon Henein[1]

[1]*Micromechanical and Horological Design Laboratory, Instant-Lab, EPFL, Switzerland*

hubert.schneegans@epfl.ch

Abstract

Typical flexure-based XY-stages have a serial design, and their layout results in the flexures being loaded in flection in face of heavy payloads or vertical loads. This paper presents a design with zero parasitic shift in which all flexures are loaded in traction/compression, resulting in a high-precision and high-load-capacity flexure-based XY-stage. A proof-of-concept demonstrator validates the concept and numerical simulations indicates sub-micron straightness error.

Flexure, XY-stage, high precision, straightness, compliant mechanism

1. Introduction

XY-stages are standard mechanical components that provide in-plane motion and are typically implemented with rolling bearings. The precision of these systems, which lies within the micron range, can be increased by turning towards flexure-based stages. These flexures, which rely on elastic deformation of flexible elements within the mechanism, are free from friction and provide a high repeatability which is desirable for high-precision applications. Moreover, flexures have the advantage of being compatible with vacuum or clean environments. In conventional designs for flexure-based XY-stages, all the blades lie within the plane of motion [1-3]. This configuration has the disadvantage of losing its straightness when high loads are applied along the z-axis, for example when moving a heavy payload (assuming the z-axis is vertical). It is indeed advantageous to avoid parts working in flection or in overhang [4]. Several XY-stage designs with parts working in traction or compression exist in the literature [5], but these suffer from parasitic motion (which forms a straightness error). This paper provides the design of a flexure-based XY-stage with zero parasitic motion and in which all key flexures are solicited in traction or compression, resulting in a high load capacity and high stiffness-to-load properties.

2. Kinematics of the mechanism and working principle

The two sources of inspiration for this design will be introduced and will then be combined to form the presented mechanism. Its mobility, internal degrees-of-freedom and overconstraints will be studied using Grubler's method. The design will then be further modified to improve its load capacity, compactness, and manufacturability.

2.1. Sources of inspiration

The compound linear stage is a well-known one-degree-of-freedom linear stage in which two parallel leaf spring stages are stacked in series to cancel out each other's parasitic motion. This design is underconstrained and requires a coupling lever that is connected to the base via a pivot, and whose role is to ensure proper synchronisation between the intermediate stage and end-effector, as shown in Fig. 1. A connecting rod is also required between the coupling lever and both the intermediate stage and end-effector. Their role is to impose the lever's x-motion to the end-effector and intermediate stage while tolerating relative z-motion and pivoting.

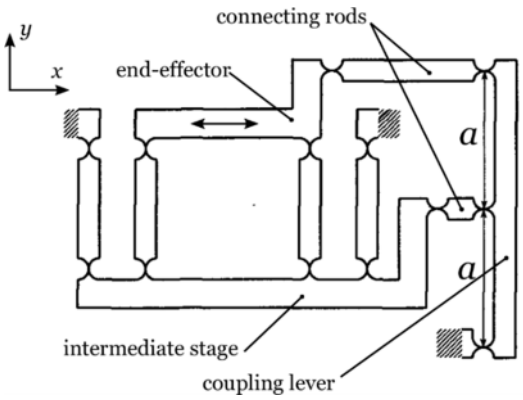

Figure 1. coupled compound flexure linear stage. This is a one-degree-of-freedom mechanism in which the end-effector moves along the x-axis.

The second source of inspiration is the three-rod-XYθ-stage presented in [6] (Fig. 2). This design allows planar XY-motion and z-rotation but suffers from a parasitic straightness error due to beam shortening.

2.2. Working principle

The presented design consists of two stacked three-rod-XYθ-stages which are synchronised with a central coupling lever, effectively creating a coupled compound XY-stage. The particularity of this slaving mechanism is that the coupling lever must now be linked to the base via a tip-tilt joint (allowing rotation around the x- and y-axes), and an equivalent to the connecting rods must be implemented which imposes both the x- and y- motion of the coupling lever to the end-effector and intermediate stage, while still tolerating relative z-motion and tilting. The tip tilt joint consists of a flexure CV-joint presented in [7] and the connecting rod equivalent is implemented with three

coplanar flexible rods. The working principle of the mechanism can be seen in Fig. 3.

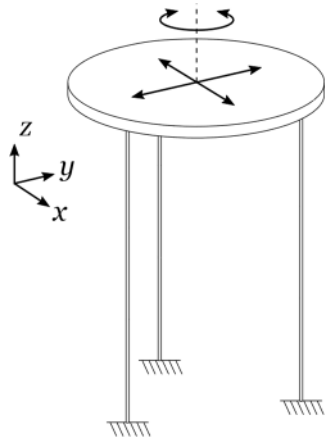

Figure 2. three-rod-XY-stage, allowing planar xy-motion as well as rotation around the z-axis.

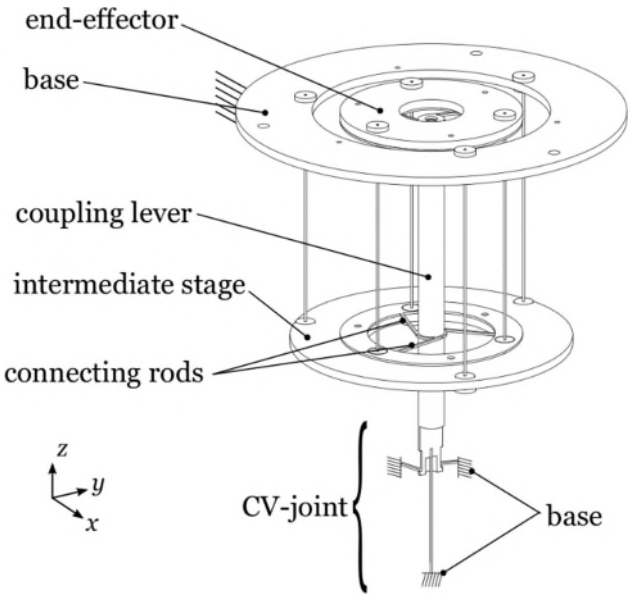

Figure 3. Overview of the mechanism. The CV-joint is a sectional view and therefore only three of its four flexible rods are visible.

2.3. Mobility, degrees-of-freedom and overconstraints of the XY-stage

The structure's mobility is evaluated using Grubler's method. The mechanism's rods can be seen as joints with five degrees-of-freedom [5]. The resulting mobility M is given by:

$$M = 6n - \sum_{i=1}^{j}(6 - f_i) = 2,$$

with $n = 3$ being the number of moving parts, $j = 16$ being the number of joints (i.e. the number of rods) and $f_i = 5$ being the degrees-of-freedom of each rod.

The mechanism has therefore two degrees-of-freedom and is free from overconstraints and internal degrees-of-freedom.

To help the understanding of the mechanism, the rigid parts and their connectivity is shown schematically in Fig. 4:

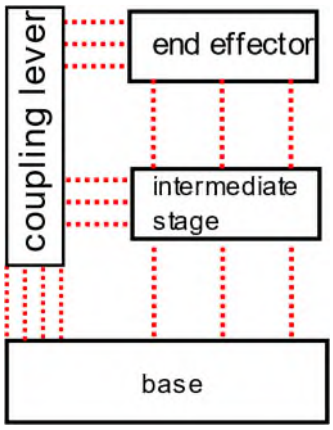

Figure 4. Summary of rigid parts and joints connecting them. The joints, represented by the red dotted lines, all consist in wire-flexures (i.e. rods, 5-degree-of-freedom linkages).

2.4. Improved flexure design

Even though the design shown in Sect. 2.3 is exactly constrained, it lacks compactness and does not have a large load capacity. Indeed, even though the six vertical rods are loaded in traction and compression, their slenderness prevents them from sustaining vertical loads efficiently.

It can also be seen in Fig. 3 that the fixed base is present in two locations: once linked to the intermediate stage, the other linked to the coupling lever. This base spanning a large distance is detrimental for precision but is best to find compact designs [4].

The improved version results in the structure shown in Fig. 5:

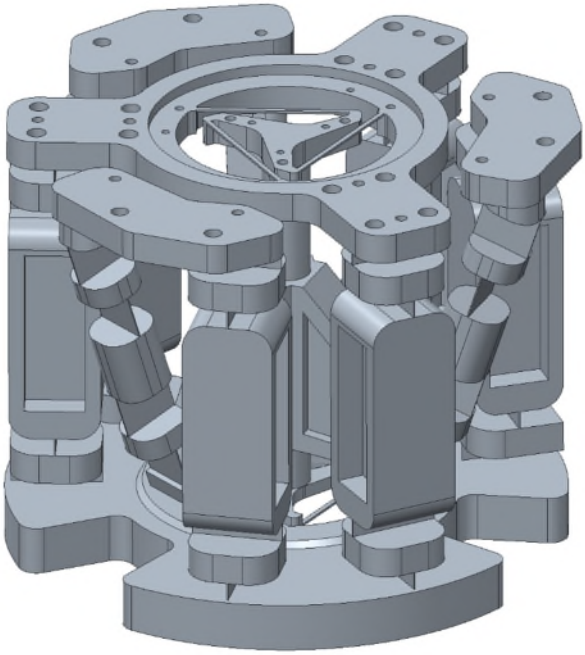

Figure 5. Overview of the improved design. The ground is in three parts which are then all fixed to a plate (not shown here).

The six vertical rods are replaced by legs consisting of two pairs of stacked blades. Each pair of stacked blades acts as a two-degree-of-freedom universal joint and increases the load capacity and stiffness-to-load [5].

The coupling lever is shortened by opting for a remote centre of compliance (RCC) ball-joint, highlighted in Fig. 6. This ball-joint is based on [8], in which the flexible rods are again replaced by stacked blades. The advantages of this RCC design are its compactness and that it shares the same base as the six vertical

rods. This joint no longer blocks torsion around the z-axis and the end-effector now has three degrees-of-freedom: XY-planar motion and a z-rotation.

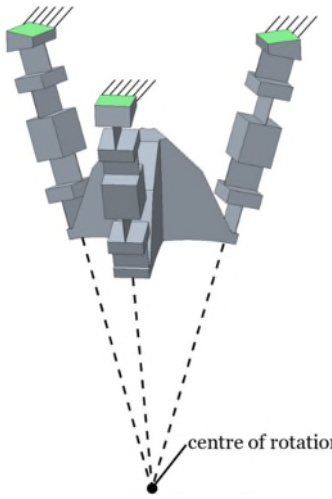

Figure 6. Highlight of the RCC coupling lever with its remote centre of rotation.

3. Demonstrator prototypes

The complexity of this design is a good opportunity to showcase the benefits of additive manufacturing. A first cheap demonstrator prototype is constructed out PA12 (Nylon) by SLS, on which the straightness of motion was experimentally measured. A second prototype made of steel and printed by SLS is currently underway, for which the numerical results for straightness and stiffness-to-load will be shown.

3.1. PA12 demonstrator prototype

The constructed demonstrator prototype out of PA12 is shown in Fig. 7:

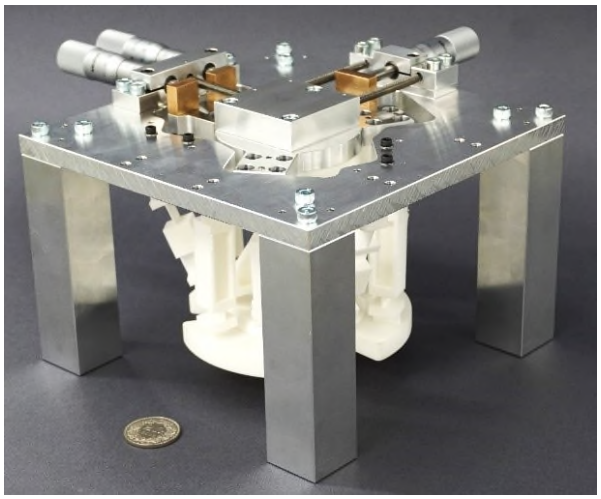

F**igure 7.** picture of the PA12 3D-printed prototype.

The XY-stage is actuated by means of three manual micrometric screws (as there are three degrees-of-freedom) with preloading springs to ensure contact between the screws and the end-effector. The straightness error was measured in a preliminary manner using a height measuring gauge, suggesting as straightness error of +-3 um. In the setup, the XY-stage was fixed to a reference Granit surface plate and the height gauge measured the z-motion of the end-effector (always on the same target fixed to the end-effector). Moreover, the linear component in the measured height was removed, as it is not a straightness error, but comes from the plane of motion not being parallel to the Granit surface plate. After inspection however, the repeatability of the measurement was also in the range of +-3 um, meaning that a more precise measurement setup should be considered. Though the numerical values of this experiment are inconclusive, they show that the low-cost prototype is still able to provide a straightness in the order of a few microns.

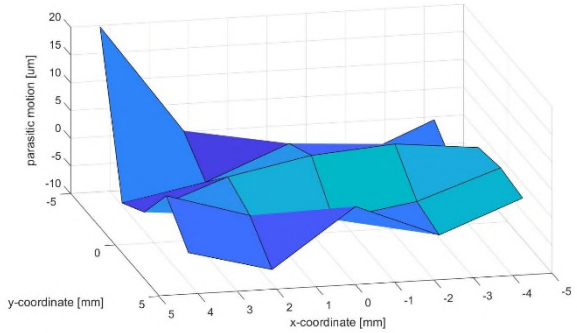

Figure 8. Measured straightness error of the PA12 demonstrator prototype. Note: the value at +20 um is most likely a measurement error, suggesting a straightness error of +-3 um.

3.2. Steel 3D-printed prototype

The second, higher quality, steel 3D-printed prototype is currently under fabrication and is shown in Fig. 9. The printing of the connecting rods is difficult for this technique as they are horizontal. For this reason, only the vertical legs and the RCC coupler are printed. The connecting rods and end effector are then added during assembly.

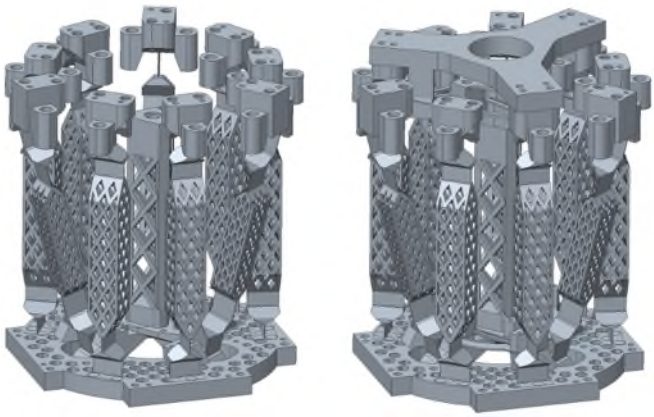

Figure 9. Left: 3D-printed part
Right: After assembly of the connecting rods and the end-effector.

The expected straightness error for the end-effector has been estimated by simulating a selection of vertical loads (in the (-z) direction). For simplicity, the stage was displaced in a single direction, therefore using only one of its two degrees-of-freedom. The results are shown in Fig. 10. It should be noted that the simulation considered geometric non-linearities.

To reduce the computation time and simulation complexity, only the flexible elements were simulated, assuming the rest of the parts as infinitely rigid, as shown in Fig. 11.

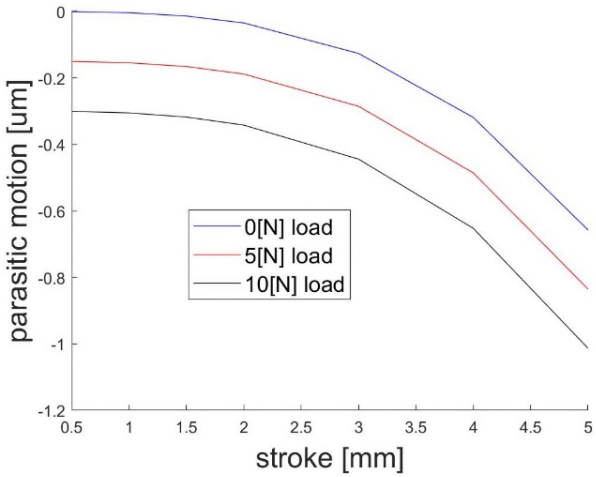

Figure 10. Simulated parasitic motion of the end effector for the steel 3D-printed stage for a selection of vertical compressive loads.

The parasitic motion lies within 0 to 1 micron for loads up to 10 N, corresponding to a straightness error of +-0.5 um. It can also be seen that the straightness errors for the 0 N and 10 N loads have an almost constant difference of 0.3 um. Last, even for zero load, the straightness error is roughly parabolic.

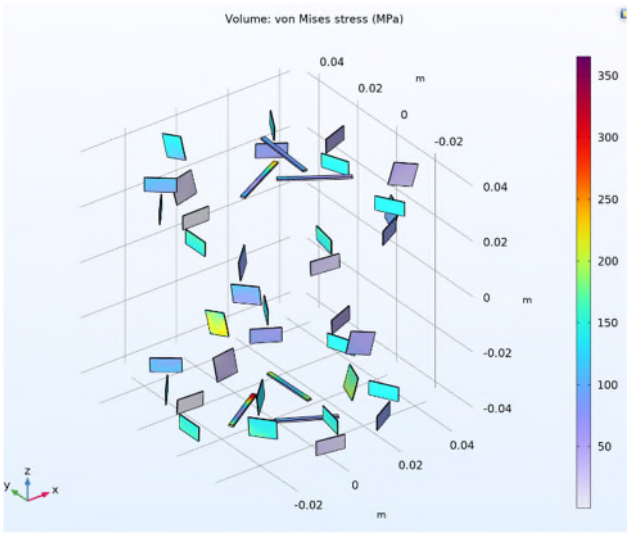

Figure 11. FEM simulation (COMSOL) of the XY-stage at 5 mm stroke. It can be seen that only the flexible elements are simulated and that the stress does not exceed 350 MPa.

4. Discussion

The PA12 demonstrator prototype validates the concept of the kinematics, as it was shown experimentally that the straightness error is within several microns. This demonstrator also highlighted the need for a more precise measurement setup, as the straightness error is within the measurement noise.

The simulated metal further consolidates the concept by reaching a straightness error of +-0.5 um for loads up to 10 N. It should be noted however that the performances will be lower for a physical prototype, as the connecting parts are not infinitely rigid and as there will misalignments between the parts.

Moreover, the small vertical shift of 0.3 um between the non-loaded and 10 N loaded stage shows how this design is well suited to move heavy objects with little loss of straightness.

Lastly, the straightness error may yet be further improved by adjusting the position of the connecting rods as these will adjust the quadratic straightness error of the stage.

5. Conclusion

This paper presented the concept, design, and kinematics of a flexure-based XY-stage. The particularity of this design is that it follows a planar motion with high-precision and that its load-bearing flexures are all solicited in traction/compression. This last property is what allows the stage to withstand higher vertical loads and to have a high stiffness to these loads.

Future work includes fabricating the steel 3D-printed prototype. It will also be necessary to implement a new measurement procedure as it was highlighted by the PA12 demonstrator. Actuation will be a key issue for the automation of this stage.

Acknowledgements

The presented design is protected under patent EP21179030.8, for which the authors are open to licensing opportunities. The authors would like to thank EPFL's Technology Transfer Office for their support as well as Dr. Sébastien Lani's guidance in the 3D-printing process.

References

[1] Piyu Wang, Qingsong Xu, Design of a flexure-based constant-force XY precision positioning stage, Mechanism and Machine Theory, Volume 108, 2017, Pages 1-13, ISSN 0094-114X, https://doi.org/10.1016/j.mechmachtheory.2016.10.007.

[2] Zhang, Zhen & Yan, Peng & Hao, Guangbo. (2017). A Large Range Flexure-Based Servo System Supporting Precision Additive Manufacturing. Engineering. 3. 708-715. 10.1016/J.ENG.2017.05.020.

[3] Wang, W., Han, C., & Choi, H. (2011). 2-DOF kinematic XY stage design based on flexure element. 2011 IEEE International Conference on Mechatronics and Automation, 1412-1417.

[4] Reymond, Clavel & Bérangère, Le & Bouri, Mohamed. (2011). Ultra-High Precision Robotics: A Potentially Attractive Area of Interest for MM and IFToMM. 10.1007/978-94-007-1300-0_37.

[5] Conception des structures articulées à guidages flexibles de haute précision, Henein, Simon, 2000

[6] Fluckiger, P, Vardi, I, & Henein, S. "Design of a Flexure Based Low Frequency Foucault Pendulum." Proceedings of the ASME 2020 International Design Engineering Technical Conferences and Computers and Information in Engineering Conference. Volume 10: 44th Mechanisms and Robotics Conference (MR). Virtual, online. August 17–19, 2020. V010T10A002. ASME. https://doi.org/10.1115/DETC2020-22075

[7] I. Vardi, L. Rubbert, R. Bitterli, N. Ferrier, M. Kahrobaiyan, B. Nussbaumer, S. Henein, Theory and design of spherical oscillator mechanisms, Precision Engineering, Volume 51, 2018, Pages 499-513, ISSN 0141-6359, https://doi.org/10.1016/j.precisioneng.2017.10.005.

[8] M. Naves, R.G.K.M. Aarts, D.M. Brouwer, Large stroke high off-axis stiffness three degree of freedom spherical flexure joint, Precision Engineering, Volume 56, 2019, Pages 422-431, ISSN 0141-6359, https://doi.org/10.1016/j.precisioneng.2019.01.011.